A Model for the Calculation of Shear Crack Widths for Beams Constructed using High Strength Steel Stirrups

Stephen Foster[1], Ahsan Parvez[2], Evan Bentz[3], Anthony Ng[4] and Graeme McGregor[5]
[1]Professor and Dean, Faculty of Engineering, UNSW Sydney, NSW, Australia
[2]Lecturer, Western Sydney University, Sydney City Campus, Sydney, NSW, Australia
[3]Professor, University of Toronto, Toronto, Ontario, Canada
[4]Engineering Solutions Manager, InfraBuild, Revesby, NSW, Australia
[5]Chief Engineer, InfraBuild, Revesby, NSW, Australia

Abstract: There is a growing interest in using high-strength steel (HSS) in concrete structures due to its numerous benefits, including reduced congestion, improved concrete placement, cost savings, and environmental benefits. However, as steel strength increases, serviceability limits become more crucial. Several studies have focused on understanding behaviour in shear and cracking mechanisms of reinforced concrete beams reinforced with HSS. Factors such as concrete strength, transverse reinforcement, longitudinal reinforcement, and beam section size all influence shear crack widths. Existing design codes, however, solely address tensile and flexural cracking, lacking applicability to shear crack widths. Therefore, it is essential to study shear crack behaviour and develop an accurate design model for incorporating HSS as transverse shear reinforcement. This study presents a validated model for calculating shear crack widths in RC beams, showing good accuracy in predicting cracking in reinforced concrete structures.

Keywords: High strength, steel, shear, crack width, sustainability.

1. Introduction

There is increasing interest in the use of high-strength steel (HSS) in concrete structures as it offers advantages such as reducing congestion in heavily reinforced sections, improved concrete placement, savings in labour and materials costs, and environmental benefits such as better utilisation of resources and lower CO_2-eq emissions. However, as steel strengths progressively increase, serviceability limits may become more critical.

Cracking is an important consideration in the design of a reinforced concrete (RC) member and could adversely affect a structure's serviceability performance. Early studies [1, 2] focused on tensile and flexural crack behaviour of RC members. During the last decades, several studies have been conducted to understand the shear failure behaviour and shear cracking mechanisms of RC beams. Research shows that shear crack widths can be affected by parameters such as the concrete's compressive strength [3], the amount of longitudinal reinforcement [4], the quantity, arrangement, and ratio of transverse reinforcement [5], and side face cover to the transverse reinforcement [6, 7]. Sherwood et al. [8] showed that beam section size influences the crack width, as the crack widths increases with the increasing distance from the longitudinal reinforcement.

Malm [9] noted that shear cracks could be detrimental in large structural members and suggested that crack width control may be achieved by limiting the stress increment in the longitudinal reinforcement in a passive manner. The leading international design codes offer multiple models for predicting tensile and flexural crack widths, but they do not include any models for estimating shear crack widths. Thus, in the incorporation of HSS as transverse shear reinforcement in RC beams, it is important to study the shear crack behaviour and develop appropriate, and accurate, design models.

2. Cracking behaviour of reinforced concrete beams

2.1 General

The strength model of AS3600:2018 [10] and AS5100.5:2017 [11] are based on the simplifications in Simplified Modified Compression Field Theory (SMCFT) [12]; however, while the SMCFT conveniently estimates the ultimate shear strength of structural members, it is not designed to predict the behaviour at the serviceability limit state (SLS). The crack width of RC beams at SLS can be established with some modifications to the Modified Compression Field Theory (MCFT) equations given in Table 1 [13]. Details of the proposal for this are discussed below.

Table 1. Equations of Modified Compression Field Theory [13].

1. Equilibrium equations:		
a. Average stresses:	$f_x = \rho_x f_{sx} + f_1 - v\cot\theta$	(1)
	$f_z = \rho_z f_{sz} + f_1 - v\tan\theta$	(2)
	$v = (f_1 + f_2)/(\tan\theta + \cot\theta)$	(3)
b. Stresses at cracks:	$f_{sxcr} = (f_x + v\cot\theta + v_{ci}\cot\theta)/\rho_x$	(4)
	$f_{szcr} = (f_z + v\tan\theta - v_{ci}\tan\theta)/\rho_z$	(5)
2. Geometric Conditions:		
a. Average strains:	$\tan^2\theta = (\varepsilon_x + \varepsilon_2)/(\varepsilon_z + \varepsilon_2)$	(6)
	$\varepsilon_1 = \varepsilon_x + \varepsilon_z + \varepsilon_2$	(7)
	$\gamma_{xz} = 2(\varepsilon_x + \varepsilon_2)\cot\theta$	(8)
b. Crack widths:	$w = s_\theta \varepsilon_1$	(9)
	$S_\theta = (\sin\theta/s_x + \cos\theta/s_z)^{-1}$	(10)
3. Stress- Strain Relationships:		
a. Reinforcement:	$f_{sx} = E_s\varepsilon_x \le f_{yx}$	(11)
	$f_{sz} = E_s\varepsilon_z \le f_{yz}$	(12)
b. Concrete:	$f_2 = \dfrac{f'_c}{0.8 + 170\varepsilon_1}\left[2\varepsilon_2/\varepsilon_o - (\varepsilon_2/\varepsilon_o)^2\right]$	(13)
	$f_1 = 0.33\sqrt{f'_c}/(1 + \sqrt{500\varepsilon_1})$	(14)
c. Shear stress on crack:	$v_{ci} \le 0.18\sqrt{f'_c}/\left[0.31 + 24w/(a_g + 16)\right]$	(15)

2.2 Principal Tensile Strain (ε_1)

The shear strength of concrete members is influenced by many geometric and loading effects, including percentage of reinforcement, applied moment, shear, and axial force and others. All these effects are captured in a single parameter being the average strain in the longitudinal direction, ε_x, at a given depth of the beam [12]. The larger this strain, the wider the cracks. The strain in longitudinal steel (ε_{sx}) due to moment and shear can be calculated as:

$$\varepsilon_{sx} = (M_S/d_V + 0.5V_S\cot\theta_V)/E_S A_{st} \ge 0 \qquad (16)$$

where V_s = service shear at critical section, M_s = service moment at the section where shear is being calculated, d_v = effective shear depth taken as maximum of 0.72D and 0.9d, D = total depth of the section, d = distance to centroid of longitudinal steel from the extreme compression fibre, E_s = modulus of elasticity of reinforcing steel and A_{st} = total longitudinal steel area in flexural tensile zone. It is notable that Eq. 16 is derived under the assumption that the member is already flexurally cracked. If this assumption is not yet valid, the equation may yield conservative results (flexural cracking can be readily checked using the principles of mechanics).

The critical shear occurs either at distance d_v from the support, in the case of a uniformly distributed load, or d_v from the load application location, for the case of a point load. At service loading the depth to the neutral axis (d_n) is at a greater depth in the section than at ultimate. Considering plane sections remain plane, the average longitudinal strain, ε_x, at mid depth of the section can be calculated from geometry.

In the MCFT, the average principal tensile strain ε_1 in the cracked concrete is used as a "*damage indicator*" that controls the average tensile stress in the cracked concrete. After cracking, the principal tensile stress f_1 in the concrete is related to the principal tensile strain ε_1 as given in Eq. 14 of Table 1.

The principal compressive stress f_2 is related to the principal tensile stress f_1, which can be obtained by re-arranging Eqs. 2 and 3 as:

$$f_2 = (\tan\theta_V + \cot\theta_V)v - f_1 \tag{17}$$

where v is the shear stress in the concrete and can be obtained by rearranging Eq. 2 in Table 1 as:

$$v = f_1 \cot\theta_V + \rho_z f_V \cot\theta_V \tag{18}$$

and where ρ_z = transverse reinforcement ratio, f_v = stress in transverse reinforcement. In the strength limit condition, the stress f_2 in Eq. (13) is limited by the crushing strength of the concrete, $f_{2,max}$:

$$f_2 \le f_{2\max} = f'_c/(0.8 + 170\varepsilon_1) \tag{19}$$

It is notable that crushing of the diagonal struts will not control at serviceability loads.

The principal compressive strain ε_2 can be calculated from Eq. 13 in Table 1 as:

$$\varepsilon_2 = \varepsilon_0\left(1 - \sqrt{1 - f_2/f_{2\max}}\right) \tag{20}$$

where ε_0 is the peak strain and may be approximated as equal to 0.002.

From strain compatibility, the principal tensile strain ε_1 can be related to longitudinal strain ε_x, the direction of the principal compressive stress θ_V and the magnitude of principal compressive strain ε_2 in the following manner [14]:

$$\varepsilon_1 = \varepsilon_x(1 + \cot^2\theta_V) + \varepsilon_2 \cot^2\theta_V \tag{21}$$

From Eq. 21, it is observed that with increasing ε_x and decreasing θ_V, ε_1 becomes larger.

The strain in transverse direction ε_{sz} is related to θ_V and can be obtained by rearranging Eq. 6 as:

$$\varepsilon_{sz} = \left(\varepsilon_1 - \varepsilon_2 \tan^2\theta_V\right)\Big/\left(1 + \tan^2\theta_V\right) \tag{22}$$

and the stress in the transverse reinforcement determined from Eq. 12.

2.3 Crack spacing and width

Several formulations exist in literature for assessment of crack spacing. For instance, the CEB-FIP Model Code [15] estimates the spacing between cracks as:

$$S_{m\theta} = 2(c + s/10) + k_1 k_2 d_{bl}/\rho_{ef} \tag{23}$$

where c is concrete cover, k_1 is a coefficient that accounts for bond between the reinforcement and concrete, k_2 is a coefficient that accounts for the strain distribution within the tensile zone, d_{bl} is the longitudinal bar diameter, s is the spacing between the longitudinal reinforcement and ρ_{ef} is the effective reinforcement ratio. Similarly, EN 1992 [16] adopts a modified version of Eq. 23, with:

$$S_{m\theta} = 3.4c + 0.425\, k_1 k_2 \left(d_{bl}/\rho_{ef}\right) \tag{24}$$

Deluce et al. [17] modified the CEB-FIP formulation as given in Eq. 23 to add biaxial conditions, which occur when flexural and shear are combined, as well as including beneficial effects of steel fibres. Excluding the contribution of fibres, the Deluce et al. equation for a biaxial strain condition is:

$$S_{m\theta} = 2(c_a + s_{b1}/10) + k_1 k_2 / s_{mi1} \;\le\; S_{m\theta.limit} \tag{25}$$

where c_a is the effective concrete cover, which can be taken as 1.5 times the maximum aggregate size. The parameter k_1 = 0.4 for deformed bars and k_2 is determined as $k_2 = 0.25(\varepsilon_1 + \varepsilon_2)/2\varepsilon_1$, where ε_1 and ε_2 are

the largest and smallest tensile strains in the concrete, respectively. In this study a limit is applied to the calculated crack spacing ($S_{m\theta.limit}$) and is discussed below.

For uniaxial strain condition k_2 = 0.25, s_{mi1} is the reinforcement effectiveness parameter for a biaxial strain condition and, for the case where shear reinforcement is normal to the axis of the member, can be determined from:

$$s_{mi1} = (\rho_{sl}/d_{bl})\sin^2\theta_v + (\rho_{st}/d_{bt})\cos^2\theta_v \quad (26)$$

The parameter s_{b1} is the effective longitudinal bar spacing in the principal tensile direction, and for a flexural-shear biaxial strain condition, with transverse reinforcement at 90 degrees to the longitudinal axis, is be taken as:

$$s_{b1} = \left[\sqrt{(\rho_l/A_{bl})\sin^4\theta_v + (\rho_t/A_{bt})\cos^4\theta_v}\right]^{-1} \quad (27)$$

where ρ_l and ρ_t and A_{bl} and A_{bt} are the reinforcement ratios and areas of a single bar, respectively, in the longitudinal and transverse directions, respectively, and θ_v is the angle of a rotating shear crack relative to the longitudinal axis of the member and is taken as normal to the principal tensile direction.

Collins and Mitchell [18] modified Eq. 23 to account for the influence of shear in the shear critical zone as:

$$S_{mx} = 2(c_x + s_x/10) + 0.25k_1(d_{bl}/\rho_l) \le \alpha D \quad (28a)$$

$$S_{mz} = 2(c_z + s/10) + 0.25k_1(d_{bz}/\rho_z) \le D \quad (28b)$$

where, c_x is the maximum distance from the longitudinal reinforcement (Figure 1), c_z is the maximum distance from the transverse reinforcement (taken as one-half of the distance between legs, in mm), d_{bl} is the diameter of the longitudinal reinforcement, d_{bt} is the diameter of the transverse reinforcement, s is the spacing between the transverse reinforcement, S_{mx} is the crack spacings characteristics of the longitudinal reinforcement, S_{mz} is the crack spacings characteristics of the transverse reinforcement ρ_l is the longitudinal reinforcement ratio, ρ_z is the transverse reinforcement ratio. In this study a limit of αD is placed on the longitudinal crack spacing component determined in Eq. 28a, with α taken as 1.0. In Eqs. (23) to (28), length dimensions are in mm and bar areas in mm^2.

The diagonal crack spacing is calculated from its longitudinal and transverse components as:

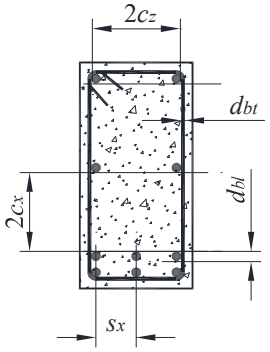

Figure 1. Definitions for crack spacing calculations.

$$S_{m\theta} = \left[(\sin\theta_v/s_{mx} + \cos\theta_v/s_{mz})\right]^{-1} \le S_{m\theta.limit} \quad (29)$$

Like that above for the Deluce et al. approach, an upper limit of $S_{m\theta.limit}$ is placed on the crack spacing.

The average crack width, $w_{cr,avg}$, is the product of the principal tensile strain and the average spacing:

$$w_{cr,avg} = S_{m\theta} \cdot \varepsilon_1 \quad (30)$$

The spacing of cracks exhibits random variation across a significantly broad range, which results in a correspondingly wide variation in crack widths. According to CEB-FIP [15], the maximum crack width can be estimated as:

$$w_{cr,\max} = 1.7 w_{cr,avg} \quad (31)$$

2.4 Model development for estimating crack widths at SLS

The mathematical relationships described through Eq. 16 to 31 are needed to predict the shear crack width using a method of iteration. The required calculations follow the methods described in Collins and Mitchell [18] and are as follows:

Step 1: Calculate service shear (V_s) and service moment (M_s) at the section where shear crack width is being calculated.

Step 2: Calculate strain in longitudinal reinforcement, ε_{sx} using Eq. 16.

Step 3: Calculate average longitudinal strain, ε_x at the mid depth of the section from geometry by calculating the depth of neutral axis, d_n.

Step 4: Estimate a value for principal tensile strain, ε_1 (a first estimate of $\varepsilon_1 = \varepsilon_x + 0.0005$ may be used).

Step 5: Estimate compressive strut angle, θ_v (as a first estimate, a value of θ_v equal to that determined for the strength may be used). In the simplified method that follows, θ_v is taken as that determined for the strength limit condition.

Step 6: Estimate stress in transverse steel, f_{sz} (an initial value of f_{sz} = 50~150 MPa may be selected, with lower values for tighter crack control).

Step 7: Calculate principal tensile stress f_1 from Eq. 14.

Step 8: Calculate shear stress, v, from Eq. 18.

Step 9: Calculate principal compressive stress f_2 from Eq. 17.

Step 10: Calculate principal compressive strain, ε_2, from Eq. 20.

Step 11: Calculate principal tensile strain, ε_1, from Eq. 21.

Step 12: Check if ε_1 (Step 11) = ε_1 (Step 4). If not, set the new value for ε_1, based on that calculated, and repeat Steps 4 to 11. Iterate until the strain calculated is within a selected tolerance.

Step 13: Calculate the transverse strain, ε_{sz} in stirrups using Eq. 22. and the stress in transverse steel, f_{sz}, from Eq. 12.

Step 14: Check if f_{sz} (Step 13) = f_{sz} (Step 6). If not, take new value for f_{sz} and repeat Steps 6 to 13. Iterate until the stress calculated is within a selected tolerance.

Step 15: Calculate the axial force N in the member based on:

$$N = A_{sx} f_{sx} + f_1 b_w d_v - V \cot\theta_v \tag{32}$$

Verify if the result for N in Step 15 is equal to the applied axial load on the member, which is usually zero. If not, calculate a new estimate for θ_v such that N equals the axial load on the member and return to Step 5. Iterate until N (or θ_v) is within the selected tolerance.

In a simplified approach, the value for θ_v is be taken as equal to that determined for the strength limit condition in accordance with AS 3600:2018 [10], and iteration on ΣN (step 15) is unneeded.

Step 16: Calculate diagonal crack spacing either from Eq. 23, 25 or 29.

Step 17: Calculate maximum diagonal crack width $w_{cr,max}$ from Eq. 30 and 31.

3. Model Validation

3.1 General

In this section, the cack width models described above are tested against a database of collected tests and given in Table 2, with crack spacings determined using the Collins and Mitchell model [18]. In addition, crack widths are calculated using the program Response-2000 [19]. In the calculations, the service load is taken as 60 percent of the failure load of the experiment.

3.2 Crack spacing

The average diagonal crack spacing for 17 beams reported in the literature, and listed in Table 2, is analysed. The longitudinal reinforcement ratio (ρ_l) varies between 0.55% and 4.1%.

In Figure 2, the average diagonal crack spacings for these beams were calculated using the approaches of Deluce et al. [17], given by Eqs. 25–27, and Collins and Mitchell [18], as given by Eqs. 28 and 29, are plotted against the longitudinal reinforcement ratio, ρ_l, in %. Figure 2a compares the models without a limitation imposed on the crack spacing to the experimental data; Figure 2b is plotted with the maximum calculated spacing taken as $S_{m\theta.limit}$ = 400 mm.

Table 2. Summary of database for validation of crack width model.

Reference	Specimens	f_{cm} (1) (MPa)	f_{sy} (2) (MPa)	$f_{sy.f}$ (3) (MPa)
[20], [21]	RM1(4), RM2(4), MR1(4), MR2(4), MR3(4), MR4(4), MM1(4), MM2(4), MM3(4), MM4(4)	48 – 53	408 – 920	426 – 830
[22], [23]	G1-M80(4), G2-M80(4)	33	830	550
[24], [25]	C-C-6, C-M-6, M-M-6(4), C-C-4(4), C-M-4(4), M-M-4(4), C-C-3(4), C-M-3(4), M-M-3(4)	27 – 33	427 – 827	427 – 827
[26]	S30-4, S40-2, S40-3, S40-4, S40-5, S40-6, S50-2, S50-3, S50-4, S50-5, S50-6, S80-2, S80-3, S80-4, S80-5, S80-6	33 – 81	530 – 554	378 – 750
[27]	B34-3, B34-5, B42-2, B42-3, B42-4, B42-5, B42-6, B68-2, B68-3, B68-4, B68-5, B68-6	34 – 68	648	334 – 667
[28]	M2-N(4), H2-N(4), N2-N, M2-S, H2-S	36 – 87	400	430

Notes: (1) f_{cm} = mean concrete strength; (2) f_{sy} = yield strength of the longitudinal reinforcement; (3) $f_{sy.f}$ = yield strength of the shear ligatures; (4) specimens where crack spacing data is reported or extracted.

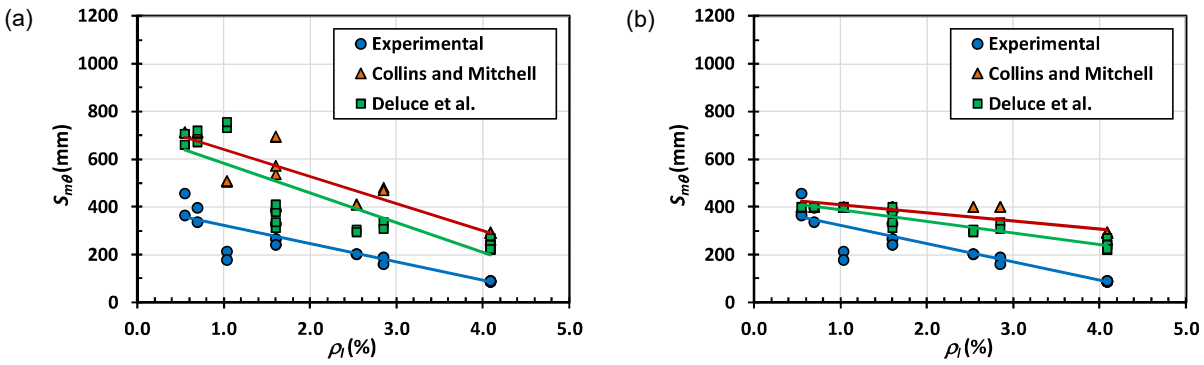

Figure 2: Longitudinal reinforcement ratio versus diagonal crack spacings: (a) no limit on calculated crack spacing; (b) with $S_{m\theta.limit}$ = 400 mm.

The findings from Figure 2 suggest that both the modified Deluce et al. [17] and Collins and Mitchell [18] models exhibit a conservative behaviour, showing that their predicted crack spacings tend to be on the safe side when compared to the experimental data (noting that larger spacing gives larger crack width; see Eq. 30).

3.3 Crack width

The shear crack model, as explained in Section 2.4, has been employed to analyse a dataset comprising 54 beams with both conventional and high-strength (HS) steel longitudinal bars and ligatures. The longitudinal bar yield strengths ranged from 400 MPa to 920 MPa, with ligature yield strengths from 330 MPa to 830 MPa. Details of the tests conducted are provided in Table 2.

To determine the crack widths, the models outlined in Section 2 were utilised; the average and maximum crack widths were calculated using Eqs. 30 and 31, respectively. The limit on the crack spacing was taken as $S_{m\theta.limit}$ = 400 mm. For each case, calculations and comparisons are made at a load corresponding to 60 per cent of the failure load of the experiment.

In addition to comparing with the model developed in this paper, we compare results with the outcomes of models analysed using the software Response-2000 [19]. In the Response-2000 analyses, the maximum crack widths are determined at the critical section for shear, specifically at a distance d_v from the applied point load, with the maximum found through the depth of the section. This typically occurred at about 60 per cent of the section's depth (measured from the top). No factor is applied to the resulting crack widths (that is crack width outputs are taken as maximum widths, not average widths).

It is found from the comparisons of the models to the test data that the analyses provide for appropriately conservative predictions of crack widths. It is also found that the simplified model with θ_v taken as that for strength performs at least as well as that of the full model, requiring one less iterative loop.

It is to be noted that the larger crack widths depicted in Figure 3 correspond to cases where HS longitudinal reinforcement is employed, resulting in higher deflections at the service load, which, in this study, is set at 60% of the failure load of the test specimens. It is improbable that HS longitudinal reinforcement can be effectively used for flexure in beams, except in cases involving stocky and non-flexural members. Of the models compared, as is to be expected, the Response-2000 model, which is based on the fully detailed MCFT, performs the best.

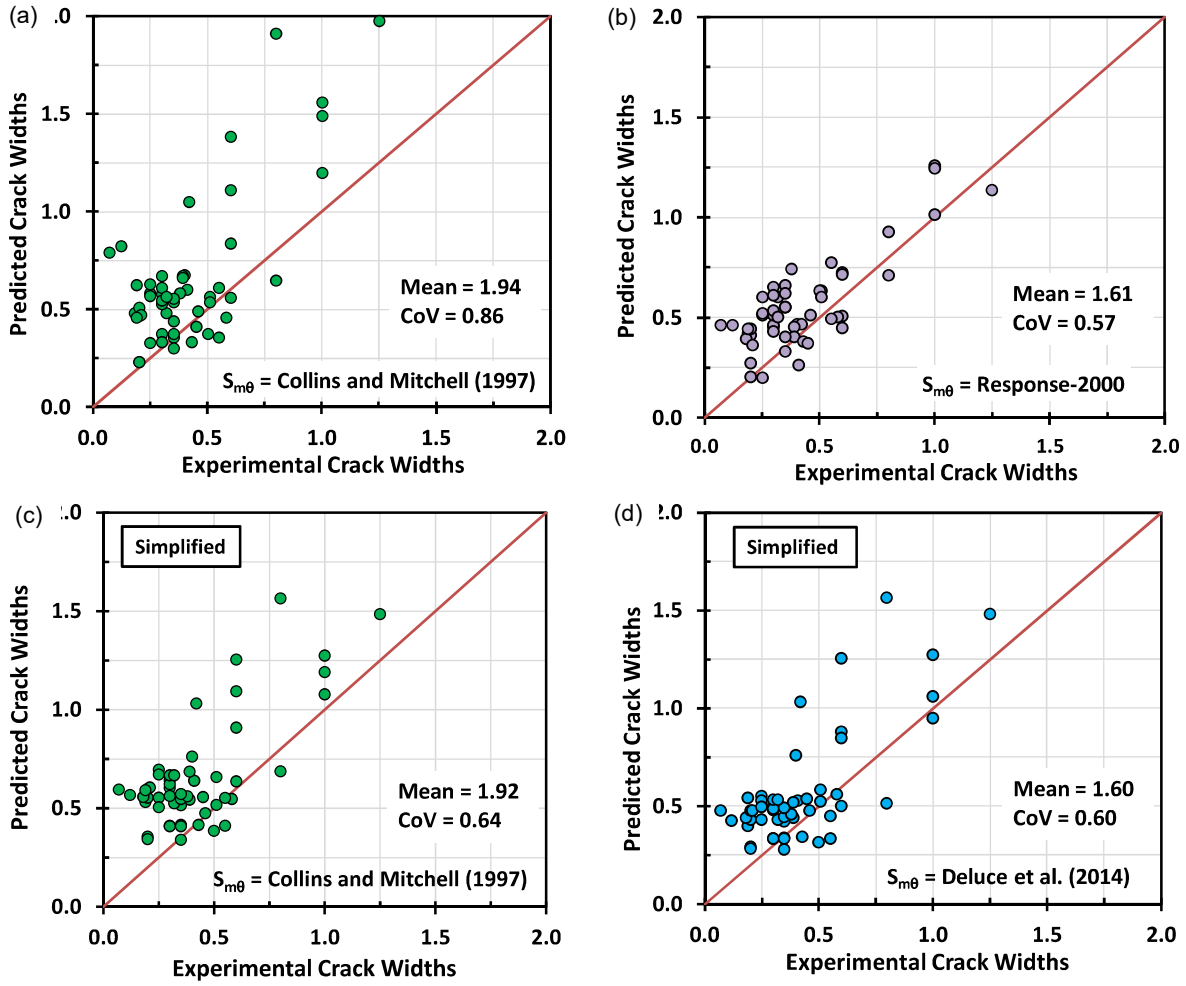

Figure 3: Experimental versus predicted crack widths: crack spacings of (a) Collins and Mitchell; (b) Response-2000; (c) and (d) Collins and Mitchell and Deluce et al. with θ_v taken as that for the ULS, respectively ($S_{m\theta,limit}$ = 400 mm).

In Figure 4 the model error (ME) for lower half data is presented on a normal probability plot for (a) the simplified approach to the Collins and Mitchell model and (b) the Response-2000 analysis. The figure shows the results to be approximately normally distributed. For the simplified Collins and Mitchell model the mean and coefficient of variation (CoV) are 1.52 and 0.27, respectively, and for the Response-2000 analysis 1.26 and 0.24, respectively. For a 75 per cent confidence of a 90 per cent characteristic crack width not being exceeded, the result from the model is multiplied by 1/[mean(ME) (1 – 1.43 x CoV)], based on n = 54 tests. For the Simplified Collins and Mitchell model, this equates to a factor of 1.07; whereas, for the Response-2000 model, the factor is 1.21.

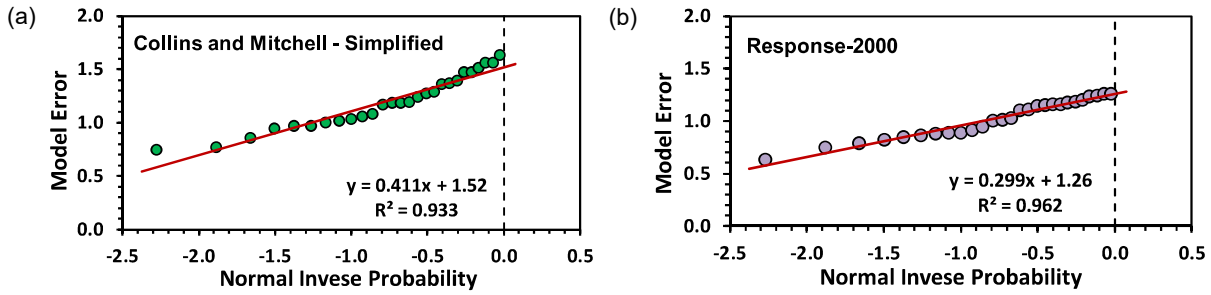

Figure 4: Model error versus normal inverse probability (a) simplified Collins and Mitchell model; (b) Response-2000.

3.4 Comments on long-term effects

Currently, there is a lack of research on the long-term effects, particularly related to creep and shrinkage, on the width of shear cracks. Despite this gap in knowledge, there have been no reported concerns regarding these effects. Creep and shrinkage are intricate phenomena known to widen the widths of flexural and imposed restraint cracks in structural elements.

In contrast to flexural elements, however, where both creep and shrinkage typically widens cracks, shear elements experience crack opening due to shrinkage and crack closing due to creep. Moreover, the Poisson effect comes into play, where creep in compressive struts between cracks tends to counteract crack widening by promoting closure. For this reason, it may be postulated that long-term influences are less important in the consideration of crack width in the shear regions of elements in flexure-shear.

4. Conclusions

The utilisation of HSS in concrete structures has gained significant attention due to its significant advantages in reducing congestion, cost savings, and environmental benefits. However, with the increase in steel strength, the importance of serviceability limits, such as crack widths, becomes more pronounced.

In this study, a validated model was presented for calculating shear crack widths in RC beams, which demonstrates reasonable accuracy in predicting complex cracking behaviour shear regions of RC beams. By addressing this aspect, the research aims to facilitate the efficient and reliable utilization of HSS in concrete construction. The Simplified Collins and Mitchell and the Response-2000 models are recommended for design.

5. Acknowledgement

This project was funded was funded by the InfraBuild; this support gratefully acknowledged.

6. References

1. Broms, B. (1965). “Crack width and crack spacing in reinforced concrete members.” ACI Journal Proceedings, Vol. 62, No. 10, pp. 1237-1256.
2. Gergely, P. and Lutz, A. L. (1968). “Maximum crack width in reinforced concrete flexural members.” Causes, Mechanisms, and Control of Cracking in Concrete, ACI, SP20, pp. 87-117
3. Piyamahant, S. (2002). “Shear behavior of reinforced concrete beams with a small amount of web reinforcement.” M. Eng. Dissertation. Kochi University of Technology, Japan.
4. Zararis, P. D. (2003). “Shear strength and minimum shear reinforcement of RC slender beams.” ACI Structural Journal, Vol. 100, pp. 203-214.
5. Witchukreangkrai, E., Mutsuyoshi, H., Takagi, M. and De Silva, S. (2006). “Evaluation of shear crack width in partially prestressed concrete members.” Proceedings of JCI, Vol. 28, No. 2, pp. 823-828.
6. Hassan, H. M., Farghaly, S. A. and Ueda, T. (1991). “Displacements at shear crack in beams with shear reinforcement under static and fatigue loadings.” Concrete Library of JSCE, Vol. 19, pp. 247-255.
7. Adebar, P. and Leeuwen, J. V. (1999). “Side-face reinforcement for flexural and diagonal cracking in large concrete beams.” ACI Structural Journal, Vol. 96, No. 5, pp. 693-704.

8. Sherwood, E. G., Bentz, E. C. and Collins, M. P. (2007). “Effect of aggregate size on beam-shear strength of thick slabs.” ACI Structural Journal, Vol. 104, No. 2, pp. 180-190.
9. Malm, R. (2006). “Shear cracks in concrete structures subjected to in-plane stresses,” PhD Thesis, Royal Institute of Technology, Stockholm, Sweden.
10. AS 3600:2018 (2018). Concrete Structures, Standards Australia, Sydney, 268 pp.
11. AS 5100.5: 2017 (2017). Bridge Design, Part 5: Concrete, Standards Australia, Sydney, 225 pp.
12. Bentz, E.C., and Collins, M. P. (2006). “Development of the 2004 CSA A23.3 Shear Provisions for Reinforced Concrete,” Canadian Journal of Civil Engineering, Vol. 33, No. 5, pp. 521-534.
13. Vecchio, F. J. and Collins, M. P. (1986). “The Modified Compression-Field Theory for Reinforced Concrete Elements Subjected to Shear,” ACI Journal Proceedings, Vol. 83, No. 2, pp. 219-231.
14. Collins, M.P., Mitchell, D., Adebar, P., and Vecchio, F.J. (1996). A General Shear Design Method, ACI Structural Journal, Vol. 93, No. 1, pp. 36-45.
15. CEB-FIP Model Code (1978). Comité Euro-International du Béton (CEB), Thomas Telford Service Ltd., London, England.
16. CEN, Eurocode 2: EN1992-1-1 (2004). “Design of Concrete Structures - Part 1-1: General Rules and Rules for Buildings,” European Committee for Standardization, Brussels, 225 pp.
17. Deluce, J. R., Lee, S. C., and Vecchio, F. J. (2014). Crack Model for Steel Fiber-Reinforced Concrete Members Containing Conventional Reinforcement,” ACI Structural Journal, Vol. 111, No. 1, pp. 93-102.
18. Collins, M.P., and Mitchell, D. (1997). “Prestressed Concrete Structures”, Response Publications, Toronto, ON, Canada, 766 pp.
19. Bentz, E.C. (2000). “Sectional Analysis of Reinforced Concrete Members,” PhD Thesis, University of Toronto, Toronto, Ontario, Canada.
20. Desalegne, A. S. (2013). Shear Behaviour of Concrete Slabs and Beams Reinforced with High-Performance ASTM A1035 Steel, PhD Thesis, University of Alberta, Edmonton, Canada, 451 pp.
21. Desalegne, A. S., and Lubell, A.S. (2015). Shear in Concrete Beams Reinforced with High- Performance Steel,” ACI Structural Journal, Vol. 112, No. 6, pp. 783-792.
22. Munikrishna, A. (2008). Shear Behavior of Concrete Beams Reinforced with High Performance Steel Shear Reinforcement, MSc Thesis, North Carolina State University, Raleigh, North Carolina, USA, 167 pp.
23. Munikrishna, A.; Hosny, A.; Rizkalla, S.; and Zia, P. (2011). “Behavior of Concrete Beams Reinforced with ASTM A1035 Grade 100 Stirrups under Shear,” ACI Structural Journal, V. 108, No. 1, pp. 34-41.
24. Sumpter, M.S. (2007), Behavior of High Performance Steel as Shear Reinforcement for Concrete Beams, MSc thesis, North Carolina State University, Raleigh, North Carolina, USA, 145 pp.
25. Sumpter, M. S.; Rizkalla, S. H.; and Zia, P. (2009), “Behavior of High- Performance Steel as Shear Reinforcement for Concrete Beams,” ACI Structural Journal, V. 106, No. 2, pp. 171-177.
26. Lee, J. Y., Choi, I. J., and Kim, S. W. (2011), “Shear Behaviour of Reinforced Concrete Beams with High-Strength Stirrups,” ACI Structural Journal, Vol. 8, No. 5, 620-629.
27. Lee, J. Y., Lee, D.H., Lee, J.E., and Choi, S. H. (2015), “Shear Behaviour of Diagonal Crack Width for Reinforced Concrete Beams with High-Strength Shear Reinforcement,” ACI Structural Journal, Vol 112, No. 3, pp. 323-333.
28. Yoon, Y. S., Cook, W. D., and Mitchell, D. (1996), “Minimum Shear Reinforcement in Normal, Medium, and High-Strength Concrete Beams,” ACI Structural Journal, Vol 93, No. 5, pp. 576-584.